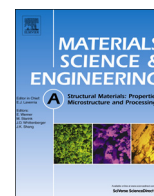




ELSEVIER

Contents lists available at ScienceDirect

Materials Science & Engineering A

journal homepage: www.elsevier.com/locate/msea

Modelling the creep behaviour of tempered martensitic steel based on a hybrid approach

Surya Deo Yadav^{a,*}, Bernhard Sonderegger^a, Muhammad Stracey^b, Cecilia Poletti^a^a Institute of Materials Science and Welding, Graz University of Technology, Kopernikusgasse 24, A-8010 Graz, Austria^b Centre for Materials Engineering, Department of Mechanical Engineering, University of Cape Town, Cape Town, South Africa

ARTICLE INFO

Article history:

Received 16 January 2016

Received in revised form

14 March 2016

Accepted 15 March 2016

Available online 16 March 2016

Keywords:

Creep

P92

Physically based modelling

Dislocations

Precipitates

Damage

ABSTRACT

In this work, we present a novel hybrid approach to describe and model the creep behaviour of tempered martensitic steels. The hybrid approach couples a physically based model with a continuum damage mechanics (CDM) model. The creep strain is modelled describing the motions of three categories of dislocations: mobile, dipole and boundary. The initial precipitate state is simulated using the thermodynamic software tool MatCalc. The particle radii and number densities are incorporated into the creep model in terms of Zener drag pressure. The Orowan's equation for creep strain rate is modified to account for tertiary creep using softening parameters related to precipitate coarsening and cavitation. For the first time the evolution of internal variables such as dislocation densities, glide velocities, effective stresses on dislocations, internal stress from the microstructure, subgrain size, pressure on subgrain boundaries and softening parameters is discussed in detail. The model is validated with experimental data of P92 steel reported in the literature.

© 2016 Elsevier B.V. All rights reserved.

1. Introduction

9–12% Cr steels are suitable candidates for fossil-fuel power plants. Due to the low procurement costs and favourable properties at high temperatures, they are used extensively in superheater tubes and boiler parts [1–6]. In order to fulfil the demand of power and the environmental safety requirements, the efficiency of power plants has to be increased as well. The efficiency of fossil-fuel power plants can be increased by raising the temperature and the pressure of the steam. Typically, power plant components are designed to operate longer than 10 years. Recently developed 9% Cr steels are suitable for temperatures up to 600 °C and pressures in the range of 30 MPa [7,8]. These operation parameters result in a reduction of 30% of CO₂ emissions when compared to subcritical power plants (540 °C/18 MPa). Current developments aim to increase the temperature and pressure limits up to 650 °C and 32.5 MPa, respectively [7,8] with a consequent reduction in the production of greenhouse gases.

In addition to creep deformation, oxidation of the material must be taken into account. The oxidation at temperatures up to 650 °C is kept low by increasing the Cr level from 9 to 12%. During recent decades, many attempts have been made to increase the Cr

content and develop 11–12% Cr steels. These steels have offered excellent short-term creep strength, but failed dramatically during long-term tests, generally after 10,000 h, due to microstructural degradation caused by the formation of modified Z-phase [7,8].

Due to the difficulties inherent in increasing the creep and oxidation resistance of these materials, gaining a detailed understanding of the underlying phenomena is of utmost importance. One step in this direction is to obtain a physical description of creep based on the microstructural evolution [9]. Several successful attempts have been made to model the creep behaviour of tempered martensitic steels. Ghoniem et al. [10] used a physically based approach including internal variables such as dislocation densities, subgrain size and precipitation state to model the creep behaviour of HT-9 martensitic steel. In other studies, the model was also used to predict the microstructure evolution of tool steel, during service [11–13]. Barkar et al. [9] used an approach whereby hard and soft regions in the microstructure were defined to describe the creep behaviour of 9–12% Cr steels. Magnusson et al. [14] used two different approaches to predict the primary and tertiary stages of creep to model the complete creep curve. Apart from these physically based models, the continuum damage mechanics (CDM) approaches have also been extensively used to model creep behaviour in these types of steels [15–18]. Basirat et al. [19] coupled the physically based model with the CDM approach to model the creep curves without taking into account the behaviour of subgrains.

All these modelling studies, which address the creep curve, have made significant contributions to this research field.

* Corresponding author.

E-mail addresses: surya.yadav@tugraz.at (S.D. Yadav), bernhard.sonderegger@tugraz.at (B. Sonderegger), strmuh001@myuct.ac.za (M. Stracey), cecilia.poletti@tugraz.at (C. Poletti).

However, there exists a lack of focus on the specific influence of internal variables involved in the modelling of creep behaviour [9–13,19,20]. For this reason, we developed a hybrid model to describe the creep behaviour using internal variables, and their evolution is analysed together with the creep curves. The coupling of physical based model with CDM is necessary to account for softening and describe tertiary creep.

In this paper, we model the creep behaviour of a steel grade P92 used in [21] applying an approach similar to that reported by Basirat et al. [19] combining a physically based model with CDM. The evolution of the variables included in the model, such as the dislocation densities, glide velocity, effective stress on dislocation, internal stress from the microstructure, subgrain size, pressure on the subgrain boundaries and softening parameters is deeply analysed.

2. Experimental data and methods

The experimental data of steel grade P92 was selected for the purpose of modelling. Creep curves, dislocation densities, subgrain size and precipitation state (type, mean radius) were discussed in the work of Ennis et al. [21] and used in our work.

Additionally, we determined the number density (m^{-3}) of precipitates, not included in [21], simulating the heat treatment for the given chemical composition with the MatCalc software. MatCalc simulates the precipitation evolution based on a Wagner-Kampmann-type model, including (i) classical nucleation theory and (ii) growth/shrinkage/coarsening/composition change based on maximum energy dissipation [22–24]. The parameters used for the MatCalc simulation are given in Table 1. The precipitates considered for the MatCalc simulation were $M_{23}C_6$ carbides, $MX_{Austenite}$ (carbonitrides formed in austenitic matrix) and $MX_{Martensite}$ (carbonitrides formed in martensitic matrix). Laves phase and modified Z-phase were not considered for the simulation because they have not been found experimentally in as received condition [21]. We assumed that the as received condition did not change during creep, although in the literature it is reported that both phases form in P92 only during ageing or creep exposure [24]. Laves phase precipitates form after 100 h and a considerable amount of Z-phase forms after 100,000 h [24].

The numerical simulations to model the creep strain (Eq. (9)) were carried out using Matlab software. The mean radius and number density of $M_{23}C_6$ obtained from MatCalc were taken as input parameters for accounting the Zener drag pressure (see Eqs. (6) and (7)). The constants and the model parameters used for the numerical simulations are provided in Appendix A.

Table 1
Parameters used for the MatCalc simulation.

| | |
|--|---|
| Thermodynamic database | mc_fe_v2.016.tdb |
| Mobility database | mc_fe_v2.001.ddb |
| Grain diameter of austenite | 60×10^{-6} (m) |
| Subgrain diameter of martensitic | 0.4×10^{-6} (m) |
| Dislocation density in austenite | 1×10^{11} (m^{-2}) |
| Dislocation density in martensite | 0.7×10^{15} (m^{-2}) |
| Nucleation sites for $M_{23}C_6$ | Grain boundaries, subgrain boundaries |
| Nucleation sites for $MX_{Austenite}$ | Grain boundaries |
| Nucleation sites for $MX_{Martensite}$ | Dislocations, grain boundaries, subgrain boundaries |

3. Model formulation

3.1. Description of the microstructure

P92 is a complex 9% Cr steel in which $M_{23}C_6$ (M=Cr and Fe) carbides are decorated along the prior austenitic grain boundaries, packet, block and subgrain boundaries. Additionally, MX-type (M=V, Nb and X=C, N) fine carbonitrides are spread throughout the matrix. Fig. 1 illustrates the microstructure of grade P92 steel in tempered condition, where different boundaries and precipitates are shown. The arrangement of different dislocations is assumed to be as shown in Fig. 1(c). The total dislocation density in the martensitic steels was therefore divided into three categories: (1) mobile dislocations ρ_m , which are free to glide under the application of a load; (2) dipole dislocations ρ_{dip} , which form dipolar or multipolar bundles; and (3) boundary dislocations ρ_b forming subgrain boundaries arranged in low energy configurations. Corresponding details can be found in the literature [10–13,19].

When materials are loaded at high temperatures with an applied stress σ_{app} , the microstructure evolves due to diffusional and relaxation processes. The glide and climb of the dislocations play important roles in the relaxation processes that occur during the dislocation creep. The microstructural evolution can be described by means of interactions such as: (a) multiplication of dislocations (Frank-Read sources), (b) immobilization of dislocations at subgrain boundaries, (c) annihilation of dislocations and (d) subgrain growth. These mechanisms were taken into account for the modelling.

The initial dislocation densities were set to $\rho_m=7 \times 10^{14}$, $\rho_{dip}=1 \times 10^{14}$ and $\rho_b=2 \times 10^{14} m^{-2}$, while a subgrain radius of 0.2 μm was chosen for the numerical simulation [21]. The partitioning of different dislocation densities was based on results reported in the literature for tempered martensite [19,25]. The fraction of dipole dislocations that are close to the subgrain boundary and transform to boundary dislocations was assumed to be 7 times less than the mobile dislocation density for simulation purposes.

3.2. Glide velocity, effective stress and internal stress

Once an external load is applied to a material at high temperature, the mobile dislocations start to move. According to Ghoniem et al. [10], the average glide velocity v_g of the mobile dislocations can be expressed as:

$$v_g = a_1 \cdot \exp[-Q/kT] [\Omega/kT] \sigma_{eff} \quad (1)$$

where Q is the activation energy for dislocation glide, k the Boltzmann constant, T the temperature, Ω the atomic volume, a_1 an adjustable parameter and σ_{eff} the effective stress. The effective stress is defined as the remaining amount of the applied stress σ_{app} available for the creep deformation and responsible for the movement of mobile dislocations over thermal barriers [9]. The expression is given as:

$$\sigma_{eff} = \sigma_{app} - \sigma_i \quad (2)$$

where σ_i describes the long-range internal stress provided by the microstructure that acts against the applied stress [26]. The internal stress has been considered differently by various researchers in the creep community. Salazar et al. [27] and Ghoniem et al. [10] used the contribution of dipoles and precipitates to describe the internal stress. Barkar et al. [9] used the mobile dislocations and precipitates to simulate internal stress in the soft region of the material. Basirat et al. [19] took into account the

Download English Version:

<https://daneshyari.com/en/article/1573467>

Download Persian Version:

<https://daneshyari.com/article/1573467>

[Daneshyari.com](https://daneshyari.com)